14.2 SIMULATING SOUTHWESTERN U.S. DESERT DUST INFLUENCES ON SUPERCELL THUNDERSTORMS

David G. Lerach
University of Northern Colorado, Greeley, Colorado

1. Introduction

Intense dust storms occur frequently within the drylands of the southwest U.S., particularly near El Paso, Texas during March, April, and May [*e.g., Novlan et al.*, 2007]. These major dust episodes often result from high winds produced over the Chihuahuan Desert [*e.g., Rivera Rivera et al.,* 2009]. Dust can be lifted to altitudes higher than 3 km above the surface ahead of frontal zones and transported regionally on a time scale of hours to a few days [*Park et al.*, 2007; *Rivera Rivera,* 2009]. This study reinvestigates the possible linkage between lofted mineral dust from the desert southwest and severe storms, using numerical modeling techniques and current theories regarding aerosol impacts on deep convection.

It has long been suggested through laboratory measurements and observations that mineral dust effectively serves as ice nuclei (IN) for heterogeneous nucleation of the ice phase in the atmosphere [*e.g., Schaefer*, 1949; *DeMott et al*., 2010]. Additionally, studies have presented evidence that small dust particles may serve as CCN once coated with soluble material [e.g., *Fan et al.,* 2004]. *Koehler et al*. [2009] found that various types of dry-generated, wettable dust particles as small as 400 nm in diameter served as CCN at typical cloud supersaturations (0.2-0.3%). Other studies have also suggested that super-micron dust may serve as giant CCN (GCCN) [e.g., *Levin et al*., 2005]. With the potential to serve as CCN, GCCN, and IN, disagreement exists over the most important pathways by which mineral dust indirectly affects clouds and precipitation [e.g., *Rosenfeld et al*., 2001; *Levin et al*., 2005].

Atmospheric aerosol can have notable indirect microphysical impacts on deep convection by serving as CCN, GCCN, and/or IN [e.g., *Khain et al*., 2004; *Seifert and Beheng,* 2006; *van den Heever et al*., 2006; *Carrió et al.,* 2010]. Multiple studies have shown that given the same liquid water content, increasing CCN number concentrations will generally inhibit collision and coalescence, and thus the warm rain process [e.g., *Gunn and Phillips,* 1957; *Borys et al*., 1998]. This effect has been numerically simulated within ordinary deep convective clouds [*Wang,* 2005; *Fan et al.,* 2007] and supercells [*Lerach et al*., 2008; *Lerach and Cotton,* 2012; *Lim and Hong,* 2010]. The initial suppression in precipitation formation may result in more supercooled water transported vertically within the updraft region, creating stronger updrafts aloft via enhanced latent heating effects from freezing [*Khain et al*., 2004; *Seifert and Beheng,* 2006; *van den Heever et al.,* 2006; *Carrió et al*., 2010]. In addition, the rapidity of glaciation in deep convective clouds is dependent upon the presence of drizzle drops and large supercooled raindrops [*Cotton,* 1972; *Scott and Hobbs,* 1977].

IN concentrations can be critical to the initial formation of hail [e.g., *Danielson,* 1977], and studies have shown that high concentrations of GCCN can promote the warm rain process via enhancement of collision and coalescence, particularly in high CCN environments [*Feingold et al*., 1999]. In deep convection, increasing GCCN and IN concentrations can enhance glaciation, which leads to further dynamical invigoration of the convective updrafts as well as increased precipitation during the latter stages of convection [e.g., *van den Heever et al*., 2006].

Aerosol influences also play an important role with respect to hydrometeor size. Numerical simulations of deep convection and supercells [*Lim and Hong,* 2010; *Lerach and Cotton,* 2012] suggest that enhancing CCN concentrations, via the reduction of warm rain efficiency, favors the production of larger hail due to greater amounts of supercooled water available for riming as well as the creation of

* *Corresponding author address: David G. Lerach, University of Northern Colorado, Dept. of Earth & Atmospheric Sciences, Greeley, CO 80639; email: david.lerach@unco.edu*

larger raindrops due to greater net liquid water paths. Consistent with the idealized numerical model results of van den Heever and Cotton [2004] and Gilmore et al. [2004], simulations favoring larger rain and hail size resulted in the production of weaker, shallower cold pools, due to the reduced net surface area of the hydrometeors and resulting reduction in evaporative cooling and melting rates [*Lim and Hong,* 2010; *Lerach and Cotton,* 2012].

In this study, numerical simulations are performed of the 15-16 April 2003 severe storms outbreak in West Texas using the Regional Atmospheric Modeling System [RAMS; *Pielke et al*., 1992; *Cotton et al*., 2003] version 6 [Saleeby and van den Heever, 2013] model to assess the role(s) that lofted mineral dust from the U.S. desert southwest might have played in the development and evolution of convection.

2. Case overview

The case chosen for this study occurred during 15-16 April 2003, when a dynamic upper level low moved rapidly from the desert southwest U.S. into the Southern Plains, resulting in rapid surface cyclogenesis in southeastern Colorado. The environmental instability in West Texas was sufficient to support severe convection after 18 UTC on 15 April (CAPE > 2500 J kg^{-1}; 0-4 km vertical wind-shear vectors > 40 m s^{-1}, or 0.01 s^{-1}; storm-relative helicity > 200 m^2 s^{-2}). As a result, the development of a well-defined dryline through West Texas triggered multiple discrete supercells after 23 UTC. What makes this case intriguing for study is that a major dust event occurred in association with the development of severe convection. A cold front propagated eastward through northern Mexico and New Mexico and triggered a major dust storm over the Chihuahuan Desert after 16 UTC on 15 April that propagated into West Texas.

This major dust event has been documented and simulated by multiple previous studies [*Gillette et al.*, 2006; *Mahler et al*., 2006; *Park et al*., 2009; *Rivera Rivera et al*., 2009], which focused solely on the dust transport. The case is relevant to the current study because the dust plume coincided with severe convection. Figure 1 depicts the time evolution of the dust plume and its interaction with the convective line of interest using GOES-10 satellite imagery. The dust plume is highlighted using the "split-window" technique [*Prata,* 1989; *Gu et al*., 2003], where the values contoured represent the brightness temperature difference (BTD) between the 12.0 and 10.7 μm channels. Optically thicker dust regions are characterized by larger BTD values. Lofted dust was first evident at 1615 UTC on 15 April (not shown), originating over the Chihuahuan Desert in northern Mexico. At 1730 UTC, the dust plume began advecting into the U.S. (Fig. 1a). By 1930 UTC, the dust plume was characterized by a distinct region of BTD values greater than 3 K while being advected through El Paso, TX northeastward into southeastern New Mexico. Weak convection initiated in eastern New Mexico at this time (Fig. 1b). At 2130 UTC (Fig. 1c), the dust plume surged eastward through New Mexico into strengthening convection located within the Texas panhandle. By 2330 UTC (Fig. 1d), the dust plume engulfed the southern end of the convective line.

3. Model setup

Simulations were performed using RAMS version 6.1.16 [*Pielke et al*., 1992; *Cotton et al.,* 2003; Saleeby and van den Heever, 2013] in a polar stereographic horizontal coordinate domain. Two two-way interactive nested model grids [*Clark and Farley,* 1984] with horizontal grid spacing of 2.5 and 0.5 km were employed (Fig. 2). The two outer-most grid (Grid 1) was used for setting up the synoptic-scale flow, lofting and advecting dust, and triggering convection. Grid 2 was used to allow for individual storm assessment. Grid 1 (2) was initiated on 15 April 2003 at 12 (22) UTC. Simulations were run for 16 hours (completed on 16 April at 04 UTC). The model was initialized with $1^o \times 1^o$ data from the Global Forecast System (GFS) model.

The basic gravity wave radiative condition [*Klemp and Wilhelmson,* 1978] was applied to the normal velocity components at the lateral boundaries of Grid 1. The Mellor and Yamada [1974] level 2.5 ensemble-averaged TKE scheme was utilized on Grid 1, while Grid 2 made use of the Smagorinsky [1963] deformation-K closure scheme with stability modifications by Lilly [1962] and Hill [1974].

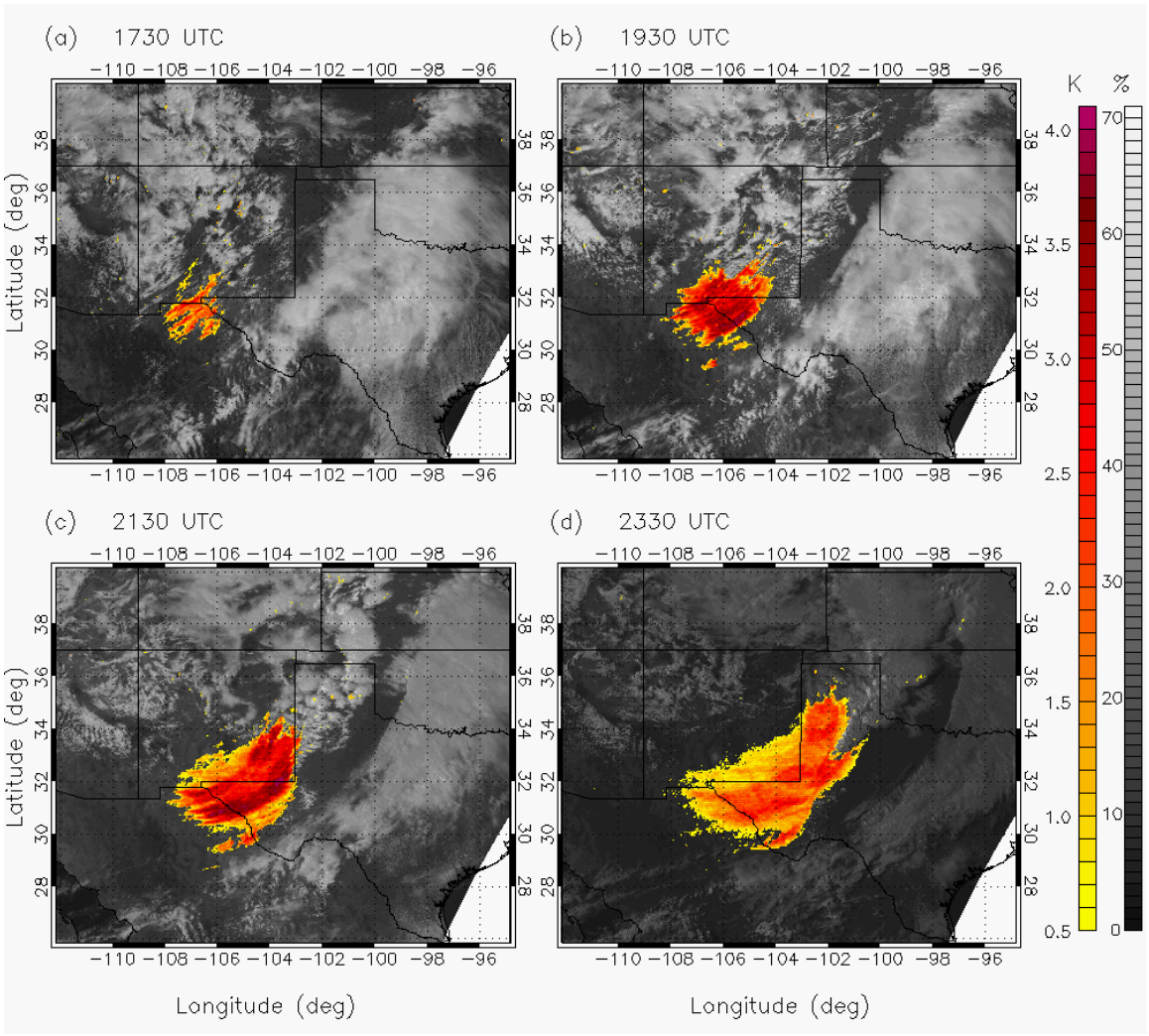

Figure 1: GOES-10 visible (albedo) imagery (black and white) overlaid with "Split window" brightness temperature differences ($T_{b,12.0\,\mu m}$- $T_{b,10.7\,\mu m}$) (colored) for (a) 1730, (b) 1930, (c) 2130, and (d) 2330 UTC on 15 April 2003.

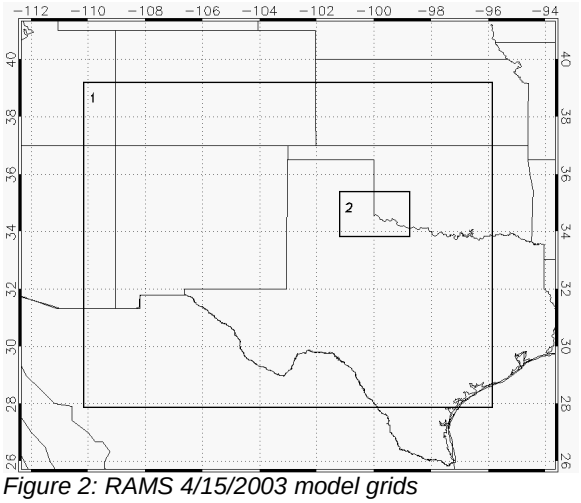

Figure 2: RAMS 4/15/2003 model grids

Each grid had 43 vertical levels spanning ~20 km; spacing increased from 50 m near the ground to a maximum of 1 km. Surface processes were parameterized using the Land Ecosystem-Atmosphere Feedback 3 model [LEAF-3; *Walko et al*., 2000]. Radiation was parameterized using Harrington's [1997]. Convection was explicitly resolved on both grids.

The dust source and transport module incorporated into RAMS for this study was based on that of Ginoux et al. [2001], which advects lofted dust in two size bins: accumulation mode and coarse mode. A bin-emulating, two-moment bulk microphysics scheme [*Meyers et al.,* 1997; *Feingold et al*., 1998; *Saleeby and Cotton,* 2004, 2008; *Saleeby and van den Heever, 2013*] was utilized in these simulations, in which the cloud droplet size distribution is decomposed into cloud droplets and drizzle drops to represent the frequently-observed bimodal distribution of cloud droplet

spectra. The scheme explicitly predicted mixing ratios and number concentrations of pristine ice, snow, aggregates, graupel, hail, cloud droplets, drizzle drops, and rain. Nucleation by CCN, GCCN, and IN was explicitly considered [*Saleeby and Cotton,* 2004].

A dust source grid was created from the MODIS 1-km Land Cover Product [*Strahler et al*., 1999] for use in this study, in order to represent the dust lofting potential of the Chihuahuan Desert and Texas panhandle croplands. The grid employed 0.2º×0.2º grid spacing and encompassed the western U.S. and northern Mexico.

RAMS background (non-dust) accumulation and course mode aerosol concentrations were initially set up as horizontally homogeneous. Initial near-surface accumulation mode aerosol were represented by concentrations of roughly 1000 cm^{-3} and a median radius of 0.035 µm, based on corresponding Weather Research and Forecasting with Chemistry (WRF/Chem) model [*Grell et al*., 2005] simulations of the event. Course mode aerosol were initialized with near-surface concentrations of roughly 0.5 cm^{-3} and median radius of 3.0 µm, based on typical continental values. The solubility fraction of such particles were set at 0.9. Dust was set up to potentially serve as CCN, GCCN, and/or IN [*Saleeby and van den Heever, 2013*], based on size, solubility, cloud temperature, and supersaturation. Heterogeneous ice nucleation was parameterized using the IN-based scheme of DeMott et al. [2010]. The accumulation (course) mode dust median radius was set to 0.2 (3.0) µm. These values were derived from limited AErosol RObotic NETwork (AERONET) observations at Sevilleta, NM (–106.885º, 34.35º) from 15 April 2003 at 2200 UTC.

Two simulations were performed. In one simulation, neither dust microphysical nor aerosol radiative effects were included. This simulation will be referred to as the control case (CTL). In another simulation, dust indirect microphysical effects were included (DST). There were no dust or other aerosol direct radiative impacts included in either simulation.

4. Preliminary Results

a. Dust plume and storm evolution

The simulated advection of the dust plume into the developing convective line (Fig. 3) corresponded well with the observations (Fig. 1). The dust plume's periphery extended ahead of the main line within the warm inflow region, where dust could be successfully ingested into the convective updrafts. Overall, the convective line evolved in a similar manner among the simulations with respect to the timing and location of convection on Grid 1. However, the DST simulation appeared to yield smaller-scale and more isolated convective cells (not shown).

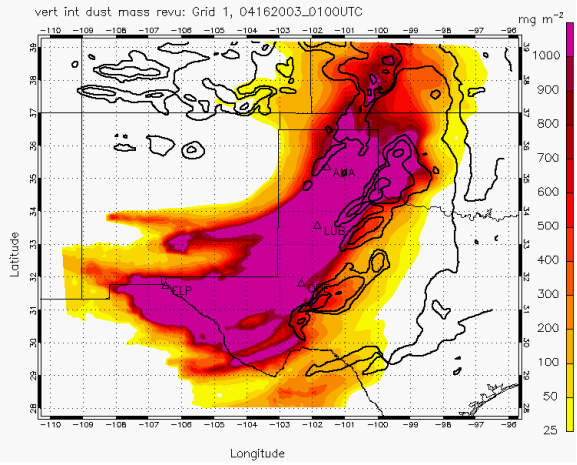

Figure 3: Simulated vertically integrated dust (color shaded) with vertically integrated condensate overlaid at 0.1, 1, and 10 mm.

The time evolution of the total condensate field at 1 km on Grid 2 is shown in Figure 4 for both simulations. Maximum 0-6 km relative vertical vorticity > 0.025 s^{-1} is overlaid. By 23:45 UTC, the DST simulation produced two storm cells exhibiting classic supercell-like characteristics, with evident mesocyclones. The CTL case produced a more linear line of convection, with a single small core of positive vertical vorticity and a larger, elongated region of mixing ratio values greater than 4 g kg^{-1}.The DST simulation continued to yield more cores of vertical relative vorticity greater than 0.025 s^{-1} than the CTL case throughout the simulation. However, the storm evolution on Grid 2 began looking similar between simulations after roughly 0 UTC on 16 April.

The convection in the DST simulation produced spatially smaller cold pools on Grid 2. While the DST simulation yielded two supercell-like storms prior to 0 UTC, the northern cell produced a notable cold pool compared to the CLN case, as the CLN case failed to produce such a storm. The southern supercell in the DST case possessed a warmer cold pool compared to the same region in the CLN simulation, which instead yielded a linear-

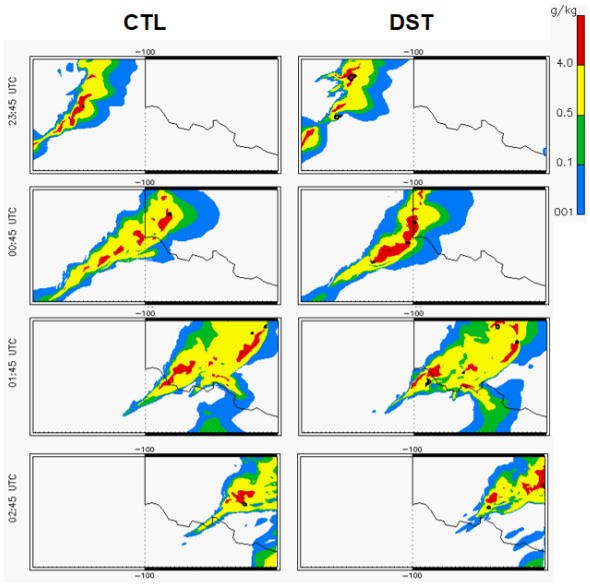

Figure 4: Simulated 1-km total condensate mixing ratio on Grid 2 (color shaded) with vertical relative vorticity > 0.025 s^{-1} overlaid.

oriented cold-pool region with surface temperature values roughly 2 – 4ºC colder than in the DST simulation. Both simulations produced cold pool regions of similar magnitude after 0 UTC, when overall convective evolution became similar (not shown).

b. Storm microphysics

The Grid-1 model environment in which convection was initially triggered on Grid 2 was characterized by average background accumulation mode aerosol concentrations of roughly 900 cm^{-3}, while mean small mode dust concentrations were around 5 cm^{-3} (maximum values were only 24 cm^{-3}). On the other hand, mean background course aerosol particle concentrations were, on average, 0.3 cm^{-3}, while mean course mode dust concentrations were double that (0.6 cm^{-3}). Maximum course mode dust concentrations exceeded 2.0 cm^{-3}, while maximum background course aerosol particle concentrations rarely exceeded 0.5 cm^{-3}. As a result, dust only accounted for approximately 2% of the model aerosol count potentially serving as CCN. However, lofted dust accounted for nearly 85% of the total course mode aerosol count, potentially serving as GCCN and IN.

Assessment of grid-cumulative hydrometeor mass on Grid 2 revealed a similar evolution between the DST and CTL simulations in the production of rain, lofted ice, graupel, and hail. The only notable differences were that the DST simulation yielded significantly more cloud and drizzle mass.

Mean profiles of rain, graupel, and hail number concentrations on Grid 2, as well as associated median diameter in updrafts greater than 1 m s^{-1}, are plotted for each simulation in Figure 5 at 23:25 UTC. Prior to 0 UTC, the DST simulation produced significantly more rain and hail than that of the CTL experiment. Graupel concentrations between simulations were similar. However, the median diameters simulated in the DST simulation were smaller than in the CTL experiment for all three hydrometeor species. Average median diameters for raindrops were 0.5 mm at 2 km above ground level (AGL) in the DST simulation and nearly double that in the CTL simulation. Average graupel median diameters were roughly 0.1 mm smaller in the DST simulation. Hail stones growing at 4 km AGL were associated with mean values of median diameter of 1.2 mm in the DST simulation. Corresponding values in the CTL simulation were closer to 1.6 mm.

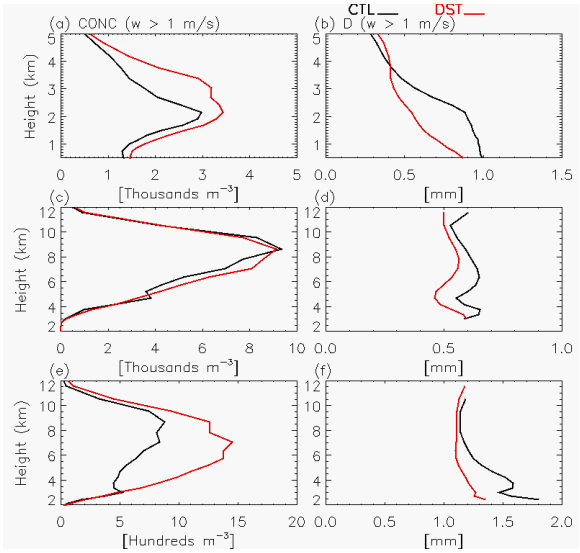

Figure 5: Mean profiles of rain (row 1), graupel (row 2), and hail (row 3) number concentrations on Grid 2 (left column) and associated median diameter (right column) in updrafts greater than 1 m s^{-1}at 23:25 UTC.

Cloud droplet and drizzle drop number concentrations and sizes were assessed for the same updraft conditions as rain, graupel, and hail (Fig. 6). Cloud droplet number concentrations and sizes evolved similarly between the simulations, with the DST experiment yielding the highest number concentrations. Note that peak cloud number concentrations at 2 km AGL were similar between simulations.

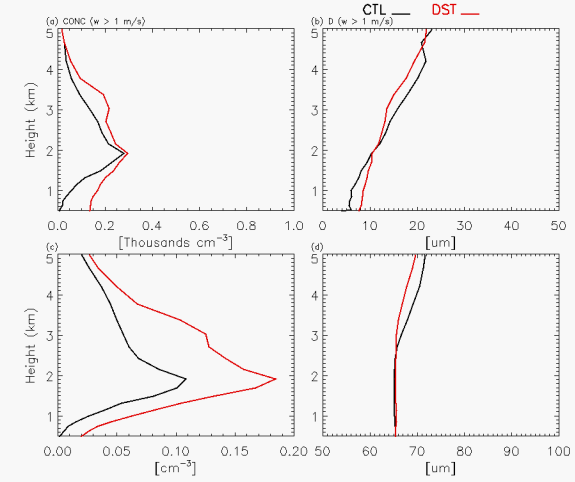

Figure 6: Mean profiles of cloud (row 1) and drizzle (row 2) drop number concentrations on Grid 2 (left column) and associated median diameter (right column) in updrafts greater than 1 m s^{-1} at 23:25 UTC.

Drizzle median diameters were similar between simulations as well, while drizzle drop number concentrations were nearly double that produced in the CTL experiment. Such differences were tied to the fact that the majority of the lofted dust mass was distributed amongst the course mode populations. Recall that the small mode dust only accounted for about 2 % of the total potential CCN population, while the large mode dust made up 85 % of the course mode potential GCCN. As a result, the small mode dust had a minor effect on initial cloud drop nucleation rates. However, the course mode dust, characterized by the same size as the background preexisting course mode aerosol, enhanced drizzle nucleation by nearly 100 % in the DST simulation compared the CLN.

After 0 UTC, the profiles of number concentrations and size for both cloud droplets and drizzle drops became quite similar between the DST and CTL simulations. This further yielded similar distributions of rain, graupel, and hail. Upon further analysis, this occurred because dust ingestion into the developing convection was cut off around this time, shutting off the ability of the dust plume to provide a source of additional GCCN.

5. Discussion

In this study, three-dimensional nested grid simulations were performed using RAMS 6 to investigate possible southwestern U.S. desert dust impacts on severe storms during the 15-16 April 2003 severe storms outbreak in West Texas. Various parameterizations were utilized in order to assess indirect microphysical effects of dust serving as CCN, GCCN, and IN.

Preliminary results suggest that accumulation mode dust serving as CCN had limited impacts on the simulated convective line, as background aerosol concentrations overwhelmed such dust populations. However, course mode dust resulted in nearly double the nucleation rates of drizzle drops. This left little to no dust remaining to serve effectively as IN, thus preventing such a process from being a major contributor to simulated differences in convection. Instead enhanced drizzle production supported the warm rain process, yielding greater number concentrations of rain but of smaller sizes than what was produced in the CLN simulation. Once lofted into the mixed phase region, this yielded a greater number of embryos for graupel and hail production. But with greater number concentrations competing for rime collection, graupel and hail grew to smaller sizes in the DST simulation. Yet the DST simulation yielded two supercell-like storms before 0 UTC while the CTL simulation managed to create a more linear line of convection with a single, weak embedded mesocyclone. At this time, the resulting cold pools produced by the supercell-like storms were warmer than those produced overall by the linear convection in the CTL experiment. This suggests that while greater rain and hail concentrations of smaller sizes were produced in the DST simulation, that these hydrometeor distributions did not lead to enhanced melting and cooling in downdraft regions, but rather enhanced glaciation aloft, stronger, dynamically stable updrafts, and more hydrometeor mass aloft that was ultimately unable to be used in precipitation processes. Additional analyses are necessary to verify this causal chain. Nonetheless, notable differences in storm severity were simulated due to lofted dust ingestion into the evolving line of convective storms, thus motivating future studies to determine the specific environments, storm types, and dust loadings necessary for dust indirect microphysical influences to be important to severe convective storm systems.

Acknowledgments

Thanks to Steve Saleeby of CSU for his assistance with the RAMS 6 model set up and Bill Cotton of CSU for motivating this study. This work was supported by National Science

Foundation (NSF) Grant ATM-0638910 and UNC Summer Support Initiative (SSI) 11308.

References

Borys, R. D., D. H. Lowenthal, M. A. Wetzel, F. Herrera, A. Gonzalez, and J. Harris, 1998: Chemical and microphysical properties of marine stratiform cloud in the North Atlantic. *J. Geophys. Res*., **103**, 22073-22085.

Carrió, G. G., W. R. Cotton, and W. R. Cheng, 2010: Effects of the Urban growth of Houston on convection and precipitation. Part I: the August 2000 case. *Atmos*. Res., **96**, 560-574.

Clark, T. L., and R. D. Farley, 1984: Severe downslope windstorm calculations in two and three spatial dimensions using anelastic interactive grid nesting: A possible mechanism for gustiness. *J. Atmos. Sci.,* **41,** 329–350.

Cotton, W. R., 1972: Numerical simulation of precipitation development in supercooled cumuli-Part I. *Mon. Wea. Rev.,* **100,** 757–763.
Cotton, R. J., and P. R. Field, 2002: Ice nucleation characteristics of an isolated wave cloud. *Q. J. Roy. Met. Soc.,* **128***,* 2417-2437.

Cotton, W. R., R. A. Pielke Sr., R. L. Walko, G. E. Liston, C. J. Tremback, H. Jiang, R. L. McAnelly, J. Y. Harrington, M. E. Nicholls, G. G. Carrio, and J. P. McFadden, 2003: Rams 2001: Current status and future directions. *Meteor. Atmos. Phys*., **82**, 5-29.

Danielson, E. F., 1977: Inherent difficulties in hail probability prediction. *Meteor. Monogr*., **16**, No. 38, Amer. Met. Soc., Boston, MA, G. B. Foote and C. A. Knight, Eds., 135-143.

DeMott, P. J., A. J. Prenni, X. Liu, S. M. Kreidenweis, M. D. Petters, C. H. Twohy, M. S. Richardson, T. Eidhammer, and D. C. Rogers, 2010: Predicting global atmospheric ice nuclei distributions and their impacts on climate. *P. Natl. Acad. Sci*. USA, **107**, 11217-11222.

Fan, J., R. Zhang, G. Li, W.-K. Tao, and X. Li, 2007: Simulations of cumulus clouds using a spectral microphysics cloud-resolving model. *J. Geophys. Res*., **112**, D04201, doi:10.1029/2006JD007688.

Fan, S.-M., L. W. Horowitz, H. L. II, and W. J. Moxim, 2004: Impact of air pollution on wet deposition of mineral dust. *J. Geoph. Res*., **31**, L02104, doi:10.1029/2003GL018501.

Feingold, G., R. L. Walko, B. Stevens, and W. R. Cotton, 1998: Simulations of marine stratocumulus using a new microphysical parameterization scheme. *Atmos. Res*., **47–48**, 505–528.

Feingold, G., W. R. Cotton, S. M. Kreidenweis, and J. T. Davis, 1999: The impact of giant cloud condensation nuclei on drizzle formation in stratocumulus: Implications for cloud radiative properties. *J. Atmos. Sci.*, **56**, 4100-4117.

Gillette, D. A., J. E. Herrick, and G. A. Herbert, 2006: Wind characteristics of mesquite streets in the Northern Chihuahuan Desert, New Mexico, USA. *Env. Fluid Mechanics*, **6**, 241-275. doi:10.1007/s10652-005-6022-7.

Gilmore, M. S., J. M. Straka, and E. N. Rasmussen, 2004: Precipitation uncertainty due to variations in precipitation particle parameters within a simple microphysics scheme. *Mon. Wea. Rev.*, **132,** 2610-2627.

Ginoux, P., M. Chin, I. Tegen, J. M. Prospero, B. Holden, O. Dubovik, and S.-J. Lin, 2001: Sources and distributions of dust aerosols simulated with the gocart model. *J. Geoph. Res*., **106**, 20255-20273.

Grell, G.A., S. E. Peckham, R. Schmitz, S. A. McKeen, G. Frost, W. C. Skamarock, B. Eder, 2005: Fully coupled "online" chemistry within the WRF model. *Atmos. Env.*, **39**, 6957-6975.

Gu, Yingxin, W. I. Rose, and G. J. S. Bluth, 2003: Retrieval of mass and sizes of particles in sandstorms using two MODIS IR bands: a case study of April 7, 2001 sandstorm in China. *Geophys. Res. Lett.*, **30**, (15), 1805. doi:10.1029/2003GL017405.

Gunn, R., and B. B. Phillips, 1957: An experimental investigation of the effect of air pollution on the initiation of rain. *J. Meteor*., **14**, 272-280.

Harrington, J., 1997: The effects of radiative and microphysical processes on simulated warm and transition season arctic stratus. Ph.D. Dissertation, Colorado State University, 289 pp.

Hill, G. E., 1974: Factors controlling the size and spacing of cumulus clouds as revealed by numerical experiments. *J. Atmos.Sci.,* **31,** 646–673.

Khain, A. P., A. Pokrovsky, M. Pinsky, A. Seifert, and V. Phillips, 2004: Simulation of effects of atmospheric aerosols on deep turbulent convective clouds using a spectral microphysics mixed-phase cumulus cloud model. Part I: model description and possible applications. *J. Atmos. Sci.*, **61**, 2963-2982.

Klemp, J. B., and R. B. Wilhelmson, 1978: The simulation of three-dimensional convective storm dynamics. *J. Atmos. Sci.,* **35,** 1070–1096.

Koehler K. A., S. M. Kreidenweis, P. J. DeMott, M. D. Petters, A. J. Prenni, C. M. Carrico, 2009: Hygroscopicity and cloud droplet activation of mineral dust aerosol. *Geophys. Res. Lett*., **36**, L08805, doi:10.1029/2009GL037348.

Lerach, D. G., B. J. Gaudet, and W. R. Cotton, 2008: Idealized simulations of aerosol influences on tornadogenesis. *Geophys. Res. Lett*., **35**, L23806, doi:10.1029/2008GL035617.

Lerach, D. G., and W. R. Cotton, 2012: Comparing Aerosol and Low-Level Moisture Influences on Supercell Tornadogenesis: Three-Dimensional Idealized Simulations. *J. Atmos. Sci.*, **69**, 969-987.

Levin, Z., A. Teller, E. Ganor and Y. Yin, 2005: On the interactions of mineral dust, sea salt sparticles and clouds – A Measurement and modeling study from the MEIDEX campaign. *J. Geophys. Res.,* **110**, D20202, doi:10.1029/2005JD005810.

Lilly, D. K., 1962: On the numerical simulation of buoyant convection. *Tellus,* **14,** 148–172.

Lim, K.-S. S., and S.-Y. Hong, 2010: Development of an effective double-moment cloud microphysics scheme with prognostic Cloud Condensation Nuclei (CCN) for weather and climate models. *Mon. Weather Rev*., **138**, 1587-1612.

Mahler, A. B., Thome, K., Yin, D., Sprigg, W. A., 2006: Dust transport model validation using satellite- and ground-based methods in the southwestern United States. In: Proceedings of the SPIE 6299, 62990L. doi:10.1117/12.679868.

Mellor, G. L., and T. Yamada, 1974: A hierarchy of turbulence closure models for planetary layers. *J. Atmos. Sci.*, **31**, 1791-1806.

Meyers, R. L., R. L. Walko, J. Y. Harrington, and W. R. Cotton, 1997: New RAMS cloud microphysics parameterization. Part II: The two-moment scheme. *Atmos. Res.,* **45,** 3–39.

Novlan, D. J., M. Hardiman, and T. E. Gill, 2007: A synoptic climatology of blowing dust events in El Paso, Texas from 1932-2005. *16th Conf. on Appl. Climatology, Amer. Meteor. Soc*., J3.12.

Park, S. H., S. L. Gong, T. L. Zhao, R. J. Vet, V. S. Bouchet, W. Gong, P. A. Makar, M. D. Moran, C. Stroud, and J. Zhang, 2007: Simulation of entrainment and transport of dust particles within North America in April 2001 (‘‘Red Dust episode’’). *J. Geophys. Res*., **112**, D20209. doi:10.1029/2007JD008443.

Park, S. H., S. L. Gong, W. Gong, P. A. Makar, M. D. Moran, C. A. Stroud, and J. Zhang, 2009: Sensitivity of surface characteristics on the simulation of wind-blown dust source in North America. *Atmos Env*., **43**, 3122-3129.

Pielke, R. A., and Coauthors, 1992: A comprehensive meteorological modeling system-RAMS. *Meteor. Atmos. Phys*., 49, 69-91.

Prata, A. J., 1989: Observations of volcanic ash clouds in the 10–12 μm window using AVHRR/2 data. *Int. J. Remote Sensing*, **10**, 751–761.

Rivera Rivera, N. I., T. E. Gill, K. A. Gebhart, J. L. Hand, M. P. Bleiweiss, and R. M. Fitzgerald, 2009: Wind modeling of Chihuahuan Desert dust outbreaks. *Atmos. Env*. **43**, 347–354.

Rosenfeld, D., Y. Rudich, and R. Lahav, 2001: Desert dust suppressing precipitation: A possible desertification feedback loop. *Proceedings of the National Academy of Sciences*, **98**, 5975-5980.

Saleeby, S. M., and W. R. Cotton, 2004: A large droplet mode and prognostic number concentration of cloud droplets in the Colorado State University Regional Atmospheric Modeling System (RAMS). Part I: Module descriptions and supercell test simulations. *J. Appl. Meteor.*, **43**, 182-195.

Saleeby, S. M., and W. R. Cotton, 2008: A binned approach to cloud-droplet riming implemented in a bulk microphysics model. *J. Appl. Meteorol*., **47**, doi:10.1175/2007JAMC1664.1.

Saleeby, S. M., and S. C. van den Heever, 2013: Developments in the CSU-RAMS Aerosol Model: Emissions, Nucleation, Regeneration, Deposition, and Radiation. *J. Appl. Meteorol Climo.*, **52**, 2601-2622.

Schaefer, V. J., 1949: The formation of ice crystals in the laboratory and the atmosphere. *Chem. Rev*., **44**, 291-320.

Scott, B. C., and P. V. Hobbs, 1977: A theoretical study of the evolution of mixed-phase cumulus clouds. *J. Atmos. Sci.*, **34**, 812-826.

Seifert, A., and K. D. Beheng, 2006: A two-moment cloud microphysics parameterization for mixed-phase clouds. Part II: Martitime vs. continental deep convective storms. *Meteor. and Atmos. Phys*., **92**, 67-82.

Smagorinsky, J., 1963: General circulation experiments with the primitive equations. I. The basic experiment. *Mon. Wea. Rev.,* **91,** 99–164.

Strahler, A., D. Muchoney, J. Borak, M. Friedl, S. Gopal, E. Lambin, and A. Moody, 1999: MODIS Land Cover Product Algorithm Theoretical Basis Document (ATBD) version 5.0. https://lpdaac.usgs.gov.

van den Heever, S. C., and W. R. Cotton, 2004: The Impact of Hail Size on Simulated Supercell Storms. *J. Atmos. Sci.*, **61,** 1596-1609.

van den Heever, S. C., G. G. Carrió, W. R. Cotton, and P. J. DeMott, 2006: Impacts of nucleating aerosol on Florida storms. Part I: Mesoscale simulations. *J. Atmos. Sci*., **63**, 1752-1775.

Walko, R. L., L. E. Band, J. Baron, T. G. F. Kittel, R. Lammers, and T. J. Lee, 2000: Coupled atmosphere-biophysics-hydrology models for environmental modeling. *J. App. Meteor.*, **39**, 931-944.

Wang, C., 2005: A modeling study of the response of tropical deep convection to the increase of cloud condensation nuclei concentration: 1. Dynamics and microphysics. *J. Geophys. Res*., **110**, D21211, doi:10.1029/2004JD005720.